# HETEROGENEOUS NANOCOMPOSITE ADHESIVE: EXPERIMENTAL TESTING AND COMPUTATIONAL MULTISCALE MODELING

BY

KEVIN SCHREADER

THESIS

Submitted in partial fulfillment of the requirements
for the degree of Master of Science in Theoretical and Applied Mechanics
in the Graduate College of the
University of Illinois at Urbana-Champaign, 2010

Urbana, Illinois

Adviser:

Professor Iwona M. Jasiuk

## ABSTRACT

This study is focused on a multiscale adhesive used for the investigation of bone bonding applications. Additionally hydroxyapatite nanoparticles were added to the adhesive to create a composite in attempts to enhance both the mechanical and biological properties. One of the main objectives was creating an adhesive system that is tailored to the biological environment in which it must operate. A solid adhesive layer as found in most engineering applications would be counterproductive to the bone healing process and thus an alternative solution was sought. A preliminary cell culture demonstrated that a polyurethane based adhesive tested was nontoxic to cells, and had the unique chemistry that would allow it to be processed into a foam. This porous structure is advantageous in a fracture healing scenario since the interconnecting pores aid in cell migration and ingrowth. This heterogeneous nanocomposite foam that is able to provide optimum conditions for the biological environment also presents additional issues that are of interest from a fundamental viewpoint. The material is composed of multiscale features with hydroxyapatite particles at the nano-scale level, and pores at the micro-scale level. This porosity and spatial heterogeneity introduces new challenges and opportunities for characterization and modeling. The experimental testing of this composite adhesive with unique characteristics then also provides support for the development of open issues in multiscale heterogeneous adhesive models.

*Dedicated to my parents and all those who nurtured*

*my intellectual development over the years.*

## Acknowledgments

This endeavor would not have been possible without the support of many people. Many thanks are due to my adviser, Dr. Iwona Jasiuk, who guided the development of my skills with great patience. I also owe thanks to Dr. Ilker Bayer, Dr. Eric Loth, Dr. Derek Milner, and Dr. Karel Matous for assistance and guidance on my projects. And finally, thanks to my family, and numerous friends who always offered me support and love throughout this process.

## TABLE OF CONTENTS

## LIST OF FIGURES

## LIST OF TABLES

# CHAPTER 1

# INTRODUCTION

## 1.1 Adhesives

The basic technology of adhesives has been a part of human kind for much of our history and is an integral part of daily life. It wasn't until the mid 20th century that the mechanics problems associated with adhesive joints, such as the non-uniform stress distributions and the resulting strong dependence of strength on geometrical parameters, began to be understood [1]. It is now a particular division of solid mechanics that incorporates the surface interaction at a material interface. At present numerous models exist that attempt to capture the behavior of adhesives within a mechanics framework. Still experimental data to verify the stress concentrations in adhesion models is difficult to obtain because of the complicated nature of direct experimental measurements [1]. Currently there still exists a need for more direct experimental support of developing cohesive models, which is addressed in the later chapters.

## 1.2 ADHESIVES FOR MEDICAL PURPOSES

The usefulness of adhesives in everyday situations has led some to inquire as to the potential applications in a biological setting. However, it quickly becomes apparent that it is significantly more challenging to develop adhesives that are suitable for applications in a living organism. The most common engineering adhesives: epoxy resins, polyurethanes, and cyanoacrylates have received the most attention. However, attempts to utilize these adhesives were plagued with failures. Epoxy resins exhibited

poor bonding in wet conditions, tissue necrosis from polymerization heat, and dubious toxicological properties [2,3]. The use of cyanoacrylates was questionable due to the toxic effects of some monomer types, higher infection rates, and low shear strength [3]. The synthetic adhesive that showed the most overall promise for adhesive application in biological specimens was polyurethane based. The use of polyurethane polymers has also received a great deal of attention for a wide range of potential *in vivo* applications including scaffolds and hard tissue replacement [4-10]. The demonstrated ability of polyurethane for use in a biological setting made it a strong candidate for the investigation of bone bonding, and ultimately was the chosen adhesive for this study.

## 1.3 BONE BACKGROUND

Bone is unlike common engineering materials; it's a composite material with diverse hierarchical structure (Fig. 1.1). The composition is primarily a soft collagen and hard apatite crystal phase. These components are assembled in such a way as to create a complex hierarchical structure that spans multiple length scales leading to a heterogeneous composite material. It also creates a relatively stiff material, on the order of 20 GPa, compared to most biological tissues. Although bone is stiff there is water and fluid within and surrounding the bone material at all times. Most importantly the primary feature that sets bone apart from most materials found in engineering is that bone is alive and will respond to external influences as it is continually changing, which can lead to some difficulties when attempting to use common engineering solutions with it.

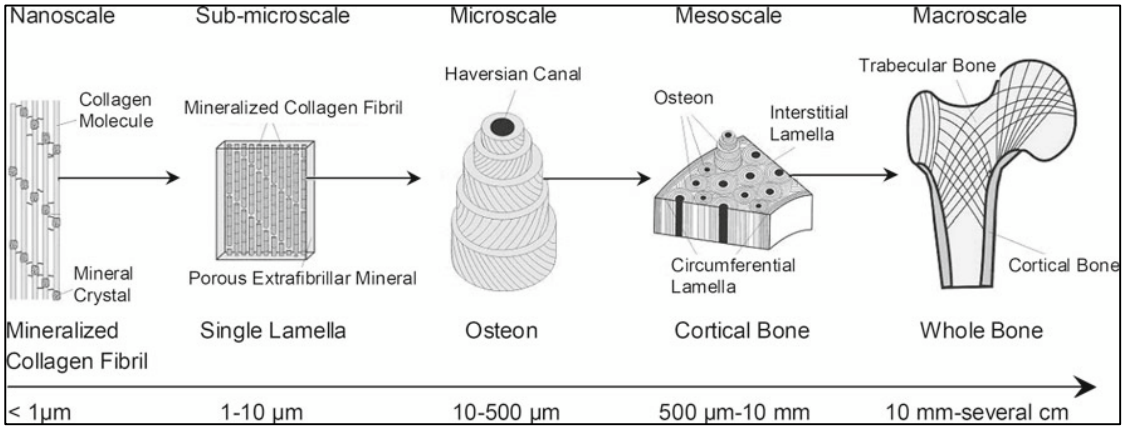


Figure 1.1. Multiscale hierarchical structure of cortical bone [11].

# CHAPTER 2

# LITERATURE REVIEW

## 2.1 STATE OF THE ART BONE FRACTURE REPAIR

Current methods for fracture stabilization in bone tissue typically require metal hardware to be affixed to the bone resulting in many challenges and limitations in this technology. The use of microsystems is particularly important in trauma surgery such as in fractures of infraorbital area, frontal sinus wall, and reconstruction of the skull [12]. The development of rigid microplates with screws in maxillofacial fractures has revolutionized treatment of related trauma, but yet many improvements are possible [13,14]. While capable of very high mechanical strength, the use of screws can result in stripping the bone due to potential over-tightening when inserted and loosening over time resulting in dislocation of the fixture, and poor anatomical healing [12]. Additional drawbacks for screws include: fractures from pilot holes, bone resorption from stress shielding, devascularization from exposure, and growth disturbance [13-15]. The resulting limitation on the tissue size and geometry with the current technology motivates the investigation of alternate techniques for bone fracture stabilization.

## 2.2 ADHESIVE ADVANCEMENTS IN BONE FRACTURE REPAIR

An adhesive bone bonding system holds potential advantages that cannot be realized with the use of metal screw systems. Because an adhesive spreads the force over a larger contact area it can be used in situations where surrounding bone material is weak or even osteoporotic [16]. Utilizing an adhesive allows the force to be transmitted throughout the contact area minimizing possible stress shielding effects

that could otherwise occur [3]. An adhesive also reduces concerns that rigid fixation may be responsible for bone atrophy due to the high stiffness of the metal plates [8].

However, unique challenges are present in the bonding of biological material in the *in vivo* conditions. Primary among these is the interface where hydrophobic polymer and hydrophilic bone come into contact [17]. In order to overcome the incompatibility between polymers and bone an amphiphilic primer can be used to modify the surface energy. The primer can decrease the barrier between the lower surface energy of polymer and the higher surface energy of hydrophilic bone surface resulting in significantly improved adhesion [13,14,17]. The composition of bone and dentin are similar with both primarily made of inorganic hydroxyapatite, the organic collagen, and water [13]. Dentin priming agents have already been well developed and thus are a natural choice for preliminary bone bonding studies that show it to be advantageous in increasing adhesion strength [13,14].

Despite challenges there are also new opportunities with the use of an adhesive fixation technique. The ideal adhesion system will provide initial stabilization and then degrade with time to allow gradual load transfer to the bone until it is finally fused. It has already been observed that enzymes appear capable of recognizing and acting on substrates such as polyurethane contributing to the degradation process [4]. An adhesive system could further work as a targeted drug delivery agent to enhance healing if bioactive compounds are incorporated within the adhesive system to promote bone ingrowth, or antibiotics to prevent infection at the trauma site [18]. It is also necessary that all parts of the adhesive system meet requirements to enable healing and prevent damage. Numerous standards have been set forth for optimum performance including:

the adhesive and its degradation products should be non-toxic, biocompatible to bone and surrounding tissue, bond in a wet environment, and have practical preparation and application [3]. These potential advantages of an adhesive fixation system make it an attractive option once all such performance requirements can be satisfied.

# CHAPTER 3

# METHODOLOGY

## 3.1 ADHESIVE MATRIX

The baseline adhesive used in this study is a methylene diphenyl diisocyanate based moisture curable polyurethane (PU) foam developed jointly by Kaneka and Nippon Polyurethane industry located in Yokohoma, Japan. The initial method investigated utilized a spray system to apply the adhesive. A large volume fraction of voids were formed during the polymerization resulting in a stiff foam like structure. This technique produced high porosity foam which limited its mechanical properties.

To address this issue, a small amount of water was added to the mixture since this is a common method for crosslinking initiation in polyurethane [7,10]. The condensation reaction that occurs with water drives the polyurea reaction and results in a release of carbon dioxide gas as a byproduct that promotes the formation of a foam structure [19]. This chosen preparation method can then yield a variety of structures that range from a foam with about 80 percent voids and 2-3 mm pores to a more dense foam with pores on the order of 200 μm in diameter. The foam structure is preferable for the use in tissue regeneration efforts with interconnecting pores to promote an ingrowth of cells and tissue [6].

One difficulty present in any undertaking involving nanoparticles is the dispersion of the particles due to the intermolecular forces that begin to dominate at that length scale. To create the composite samples hydroxyapatite (HA) was added to a small amount of water and sonicated to disperse the nanoparticles in solution. The

water was mixed with the adhesive in an ultrasound bath for a controlled time of one minute and periodically agitated to release dissolved gasses. By placing the adhesive in an ultrasound bath upon mixing the components and maintaining that stimulus for 1 minute or less in the ultrasound bath, it significantly decreased the polymerization time without the addition or modification of the chemistry of the components. The use of ultrasound during mixing resulted in a reduction of polymerization time and allowed the adhesive to achieve proper consistency for application in 10 minutes, which previously took 25 minutes. This is an important issue in a clinical application where the preparation time, and the time to achieve load-bearing strength should be minimized. At 10 minutes from initiating the reaction the adhesive obtained the consistency of a foamy paste, which proved optimal for application.

To improve biocompatibility and mechanical performance, hydroxyapatite (HA) nanoparticles of size ≤ 200 nm were added to water and sonicated before being added to samples at 1 percent concentration by volume for all of the composite adhesive samples herein. The samples were then stirred to promote shear mixing of the water with hydroxyapatite and polymer adhesive during preparation. Mechanical characterization of the adhesive was conducted in three loading modes: shear, compression, and tension as these modes are the primary types of loading that occur in the intended application environment.

### 3.2 SHEAR TESTING

To conduct the lap shear tests a polymer adherend was chosen because of the difficulty in conducting this test using bone. Also this choice allowed visual observation of the failure behavior and conformed to existing standards to make comparison of

results possible with other adhesives. Testing was carried out on an MTS Insight 2 kN testing machine with Testworks 4 used in processing test data. The shear test results were based off 5 samples in each group of polyurethane, 4 samples of bone cement, and 4 samples in each group with hydroxyapatite reinforcement. The acrylic adherend was abraded with 120 grit sandpaper in the adhesive zone and thoroughly cleaned. The ratio of polymer to water used to produce the desired porosity was 7 parts polymer to 1 part water. Once the adhesive achieved paste consistency it was applied to the acrylic adherend. The adhesive extended approximately 6.4 mm beyond the overlap length of 12.7 mm and was held in place with a 3 N clamp force according to recommendations in standard ASTM D 1002. In accordance with the standards a crosshead displacement rate of 1.3 mm/min was chosen. Afterwards bonded samples were placed in an oven at 38 degrees C for 90 minutes. The samples were tested for early properties soon after cooling or after 20 hours in ambient conditions to ensure a fully cured state.

### 3.3 COMPRESSION TESTING

Bulk compression samples to assess the load bearing capacity were prepared in 4 mL glass vials which were broken after curing. The ratio of polymer to water was used to produce desired porosity of 1 mm or less at 7 parts polymer to 1 part water. There were 2 samples of each group tested. Testing was performed with steel platens at 1.3 mm/min displacement rate to 10 percent strain.

### 3.4 BONE TENSILE TESTING

Bovine femurs of unknown age were obtained and kept frozen until processing and use. The femurs were sectioned and each piece of solid cortical bone was then

abraded on a polisher until the cross sections were roughly rectangular with typical dimensions of 6.5 mm x 18 mm x 32 mm. A precision saw was used to make a cut transverse to the longitudinal direction of the femur at 16 mm which generated the surface that was bonded. The bone was kept moist with phosphate buffer solution (PBS) throughout processing. A liquid dentin bonding primer Clearfil SE was tested as an amphiphilic agent to promote bonding with the polymer adhesive by application to the surface 10 minutes before the adhesive. A ratio of 7 to 1 polymer to water was used in the polyurethane adhesive preparation. A second group was tested using a two-part self-polymerizing PMMA bone cement with trade name Palacos R. The testing included 3 samples of polyurethane groups, 2 samples of bone cement without surface primer and 1 sample of bone cement with surface treatment. All samples were bonded under wet conditions, wrapped in PBS soaked gauze, and placed in an oven at 38 degrees C for 2 hours and 1 day time periods before testing. Flash was removed from the outside surfaces of the samples. The samples were cooled to room temperature before testing. Testing was performed with scissor grips at 1.3 mm/min displacement rate.

Titanium rods grade Ti6Al/4V obtained courtesy of Nexxt Spine with diameter 9.52 mm were bonded to the cortical bone on the outer longitudinal bone surface. The bovine cortical bone samples were cut and abraded on a polisher to flat surfaces with typical dimensions 6.5 mm x 18 mm x 16 mm. The shafts of the rods were wrapped in Teflon tape to isolate the adhesive contact area. The bone surface was treated with dentin primer applied 10 minutes before the adhesive. Each test group consisted of 3 samples. A ratio of 7 to 1 polymer to water was used in the adhesive preparation. All samples were bonded under wet conditions, covered in PBS soaked gauze, and placed in

an oven at 38 degrees C for 2 hours and were cooled to room temperature before testing. Testing was performed with scissor grips on the bone and vice grips on the metal rods with a 1.3 mm/min displacement rate.

### 3.5 CELL CULTURE ASSESSMENT

Cell tests were conducted on glass slides coated with the polyurethane adhesive. The slides were soaked in water then sterilized under UV light to remove any bacterial contaminates. The myoblast cells were put in cell growth medium on the slides and later stained with myosin heavy chain and DAPI for visual identification.

### 3.6 BIOCOMPATIBILITY ASSESSMENT

Biocompatibility testing was conducted using adult Xenopus Laevis frogs as the model because of previous data on bone defect remodeling [20]. Typical outside dimensions of the tarsus was 1 mm with bone cross-sectional area of 0.26 $mm^2$. The size limitations of the species prevented adequate study of the adhesive bonding of bone *in vivo* with available surgical techniques thus the focus remained on the biological interaction. The polyurethane adhesive was prepared with 1 percent HA by volume. The procedure included removal of a 1-1.6 mm section of the tarsus bone in the posterior limb. A blunt hypodermic needle ensured placement of 0.2 mL of adhesive into the cut section. This joint section was advantageous due to the opposing bone maintaining the mechanical stability of the limb immediately following the procedure. A total of 6 specimens were used, 2 as a control that had a tarsus section cut, and 4 that received the adhesive in the cut section. At 15 days post surgery the animals were sacrificed and prepared for cryosectioning. Sections of thickness 35 μm were obtained, and then haematoxylin and eosin stains were used for histology. Images were taken of

the sections to determine the local cellular and immunological response to the adhesive. All surgeries and animal care were performed in accordance with the University of Illinois at Urbana-Champaign Institutional Animal Care and Committee (UIUC IACUC) procedures and approved protocols.

# CHAPTER 4

# RESULTS

## 4.1 SHEAR STRENGTH

The failures were primarily adhesive in nature for all groups (Fig. 4.1). Some tests of the samples of the later abraded polyurethane and bone cement groups failed the adherends. Because of the fast cure rate the bone cement tested at 90 minutes represents nearly the full strength. Additional testing of preparation sonication time showed a decrease in strength at times exceeding 1 minute, but no negative effects for shorter times.

## 4.2 COMPRESSION STRENGTH

Compression tests yielded the elastic modulus of foam samples with and without HA particles. The compressive strength was measured at 10 percent strain (Fig. 4.2). The strain for measurement of the compressive strength was chosen based on the material behavior to be within the plateau stress region before the densification region and damage to the foam structure. The pure polymer and HA composite polymer had similar compressive strength. Using the stress strain curves a Young's modulus for both polymer and polymer HA composite were calculated (Fig. 4.3). The testing showed a lower modulus for the HA composite foam in the elastic region.

The internal structure of the polyurethane foam with and without HA particles was observed through SEM imaging. The images indicate that the polyurethane samples contain mostly regular spherical cavities of around 200 μm in diameter with interconnecting pores between cells with typical diameter of 3 μm (Fig. 4.4). The

polyurethane with HA inclusions contains more irregular voids with a greater range of size, but averaging around 250 μm in diameter with larger interconnecting pores of about 5 μm (Fig. 4.5).

### 4.3 BONE TENSILE STRENGTH

All samples showed an adhesive failure with the bone surface (Fig. 4.6). Also all unprimed bone tensile samples showed lower strength. The application of the dentin primer before the adhesive was applied demonstrated a significant increase in bond strength for all groups. Bone cement was also tested for comparison and formed weaker bonds than the polyurethane samples.

The debonding failure strength under tension for a titanium rod adhered to the bone surface was tested (Fig. 4.7). The adhesive mixed with HA resulted in a generally stronger bond force, but the degree of variance was also larger in this group.

### 4.4 CELL CULTURE

The initial cell tests were conducted on glass slides coated with polyurethane adhesive. Myoblast cells cultured in the medium on the adhesive samples were able to attach to the coated slides. The cells were stained for myosin heavy chain in green and nuclei stained with DAPI in blue for identification (Fig. 4.8). Visual inspection of the cells on the adhesive indicates they grow and differentiate at their normal rates.

### 4.5 BIOCOMPATIBILITY TESTING

Images of sections from the control and adhesive groups were taken from in and around the defect area. Some increased immunological response was visible in the adhesive samples. Adhesive is visible as a translucent material within some of the

sections between the bone and outer skin (Fig. 4.9. F and 4.9. G). Many similar normal responses were observed in the control and experimental specimens.

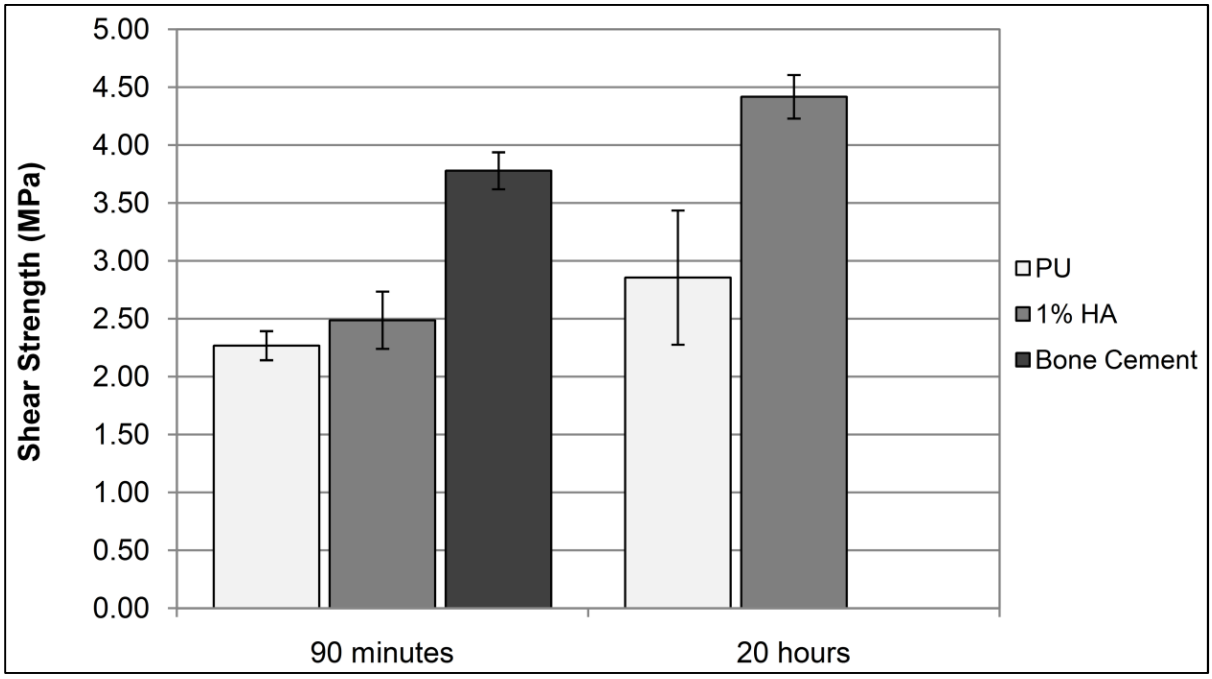


Figure 4.1. Results of lap shear tests showing ultimate shear strength of polyurethane, polyurethane with HA, and bone cement.

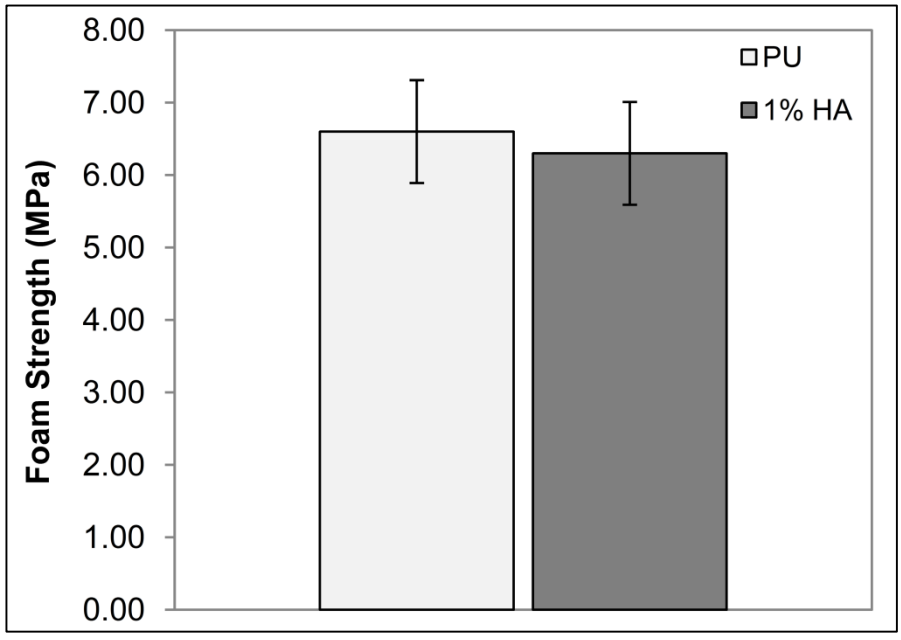


Figure 4.2. Compressive strength at 10 percent strain for polyurethane and polyurethane with HA.

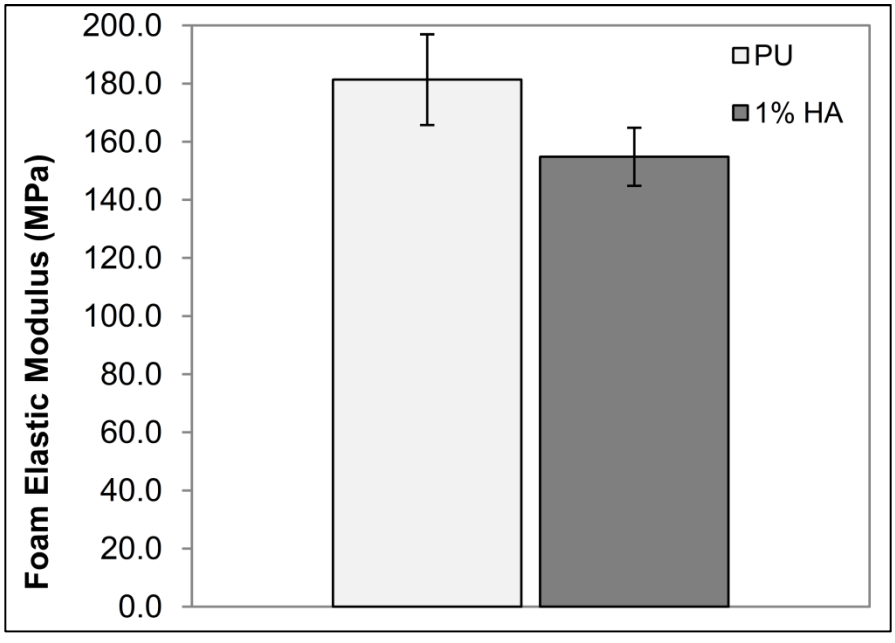


Figure 4.3. Compressive elastic modulus for polyurethane, and polyurethane with HA.

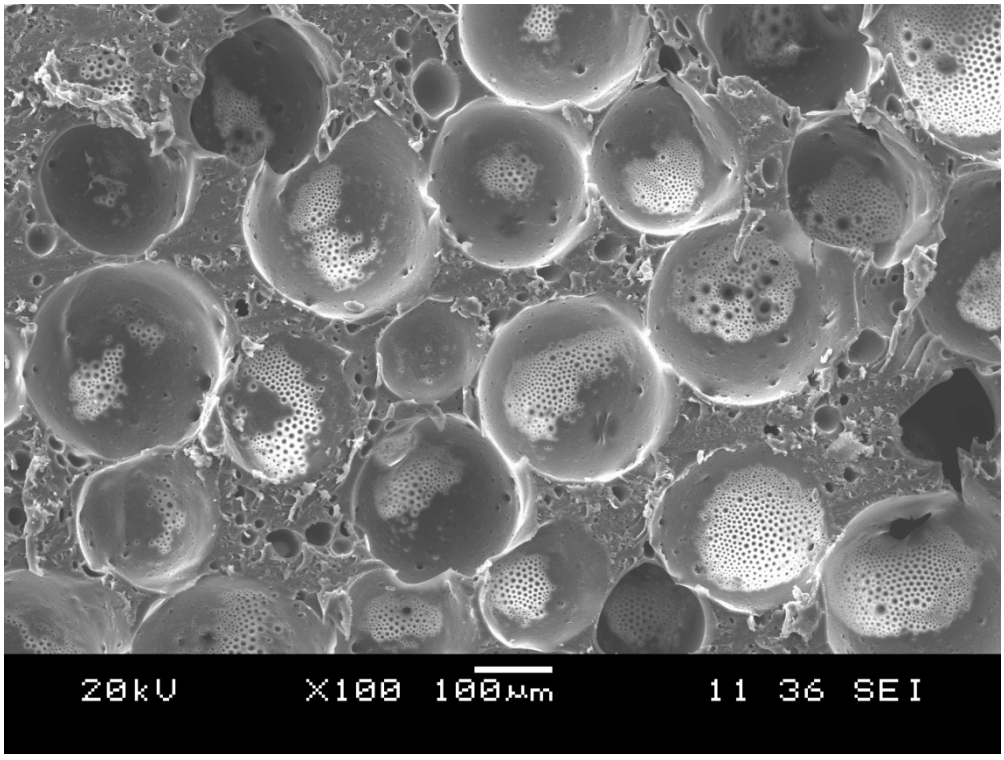


Figure 4.4. SEM image of bulk polyurethane foam section.

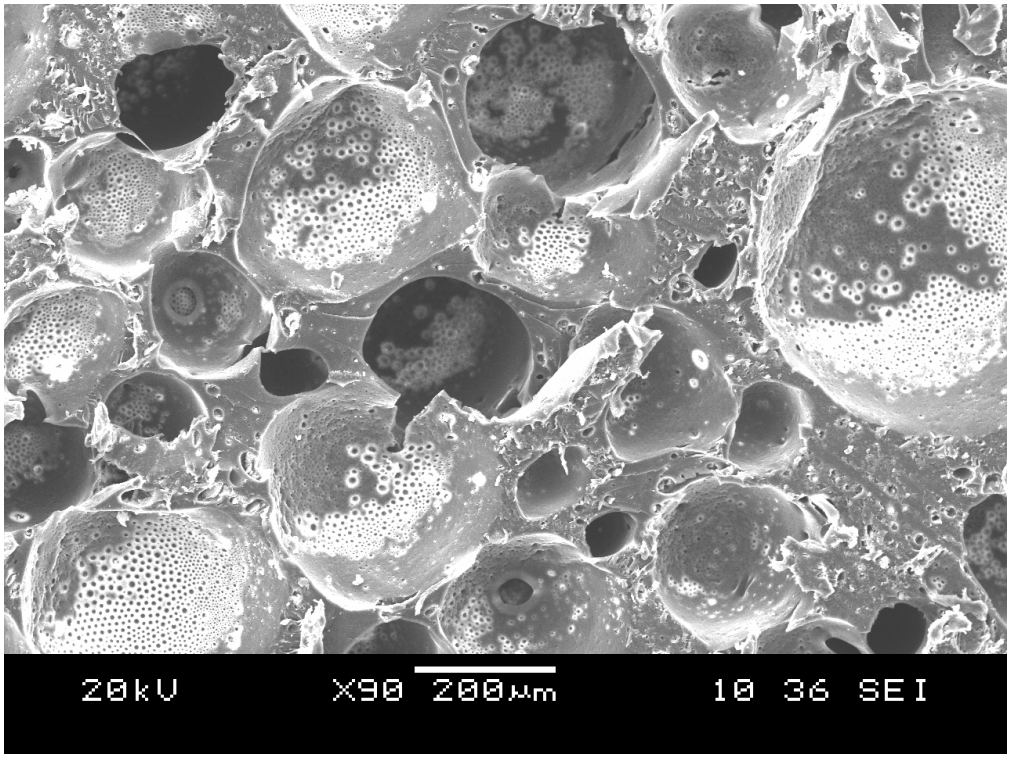


Figure 4.5. SEM image of bulk polyurethane foam section containing 1% HA.

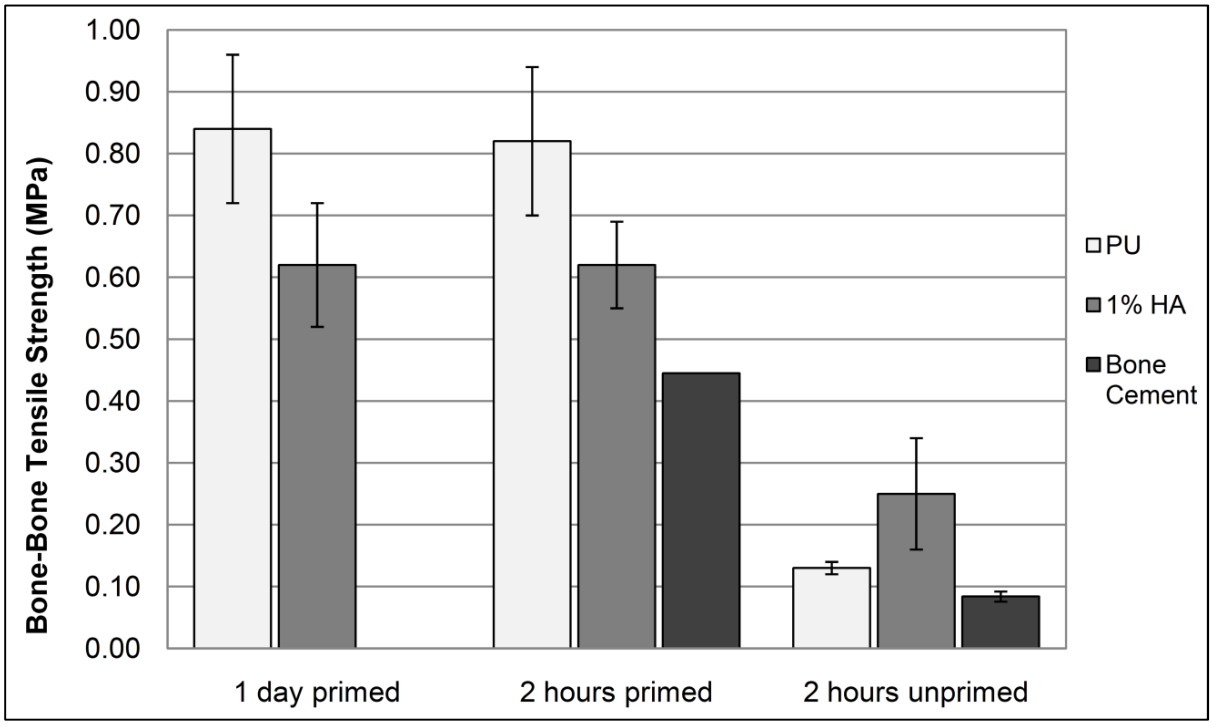


Figure 4.6. Bone-to-bone tensile bond strength for polyurethane, polyurethane with HA, and bone cement.

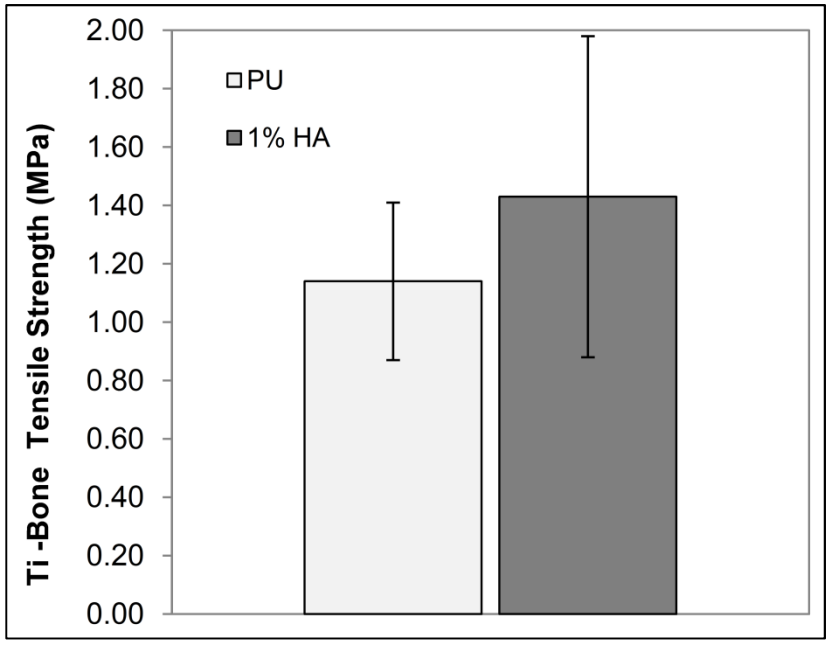


Figure 4.7. Results of bone to Ti rod bonding tests at 2 hours showing tensile strength of polyurethane, and polyurethane with HA.

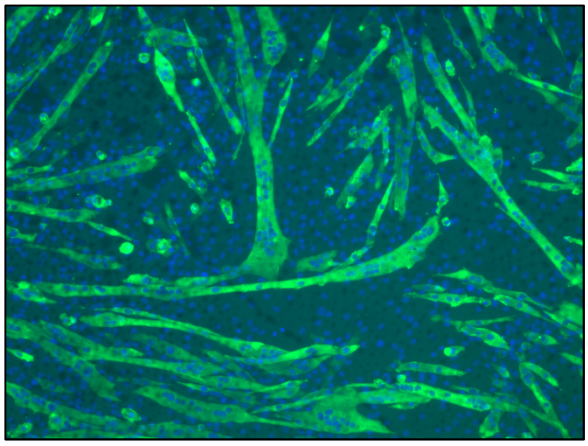

Figure 4.8. Image of Myoblast cells growing on the adhesive.
Stained for myosin heavy chain in green and nuclei stained with DAPI in blue.

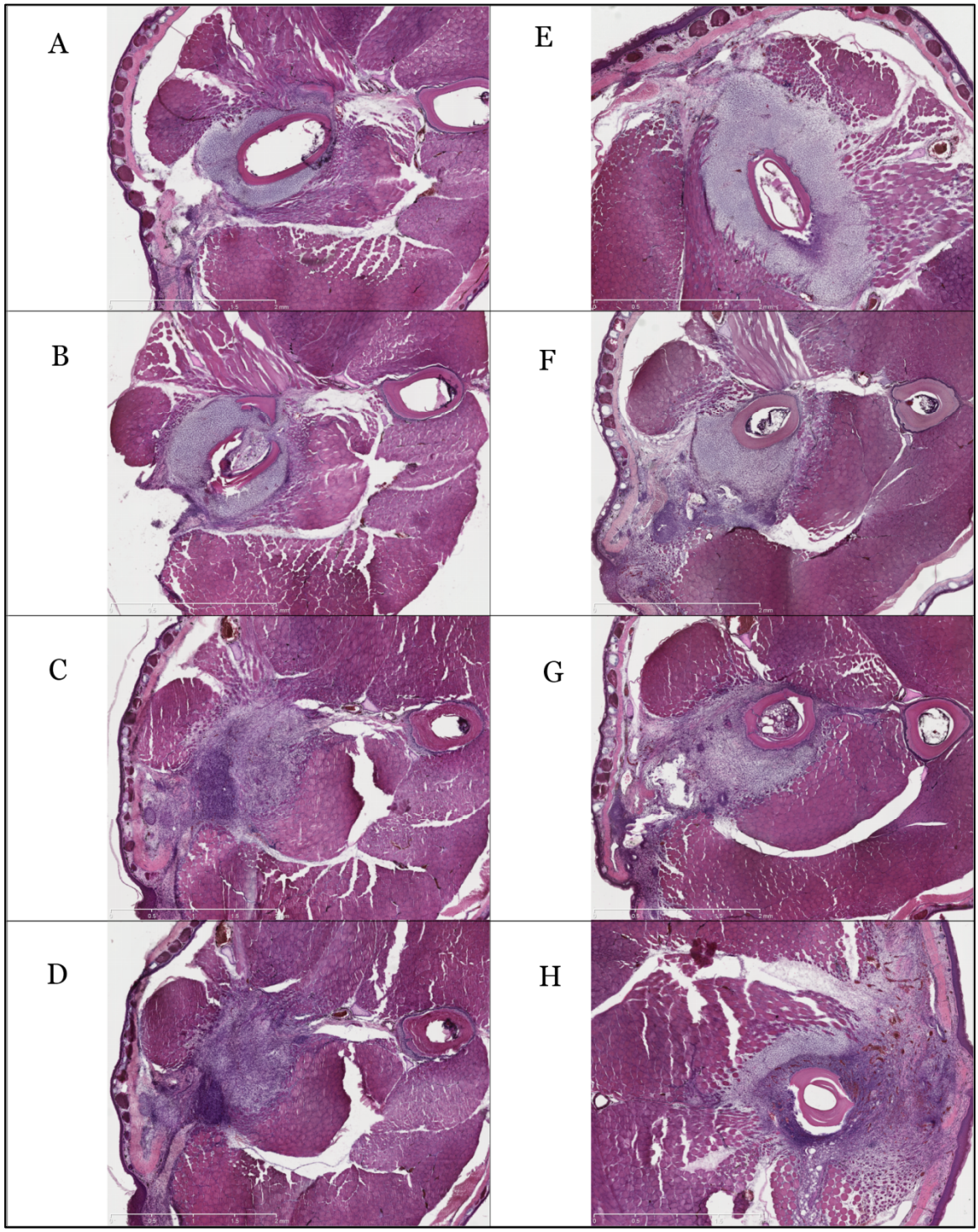


Figure 4.9. Left: Sections around bone defect site with no treatment specimens. Regions from 2 specimens are shown (A, B) and (C, D) at a range of locations along the limb.

Right: Sections around bone defect site in specimens with adhesive. Cross-sections shown include 3 of the experimental specimens (E), (F, G), and (H).

# CHAPTER 5

# DISCUSSION

## 5.1 REVIEW OF RESULTS

The shear testing demonstrated that the pure adhesive can achieve about 80 percent of its full strength within 90 minutes of application. Since the failures in the polyurethane samples were almost all adhesive in nature this result represents the ability of the adhesive to bond to the acrylic in a given time rather than the maximum cohesive strength of the adhesive developed through curing. The bone cement is chemically similar to the adherend and likely contributed to its high bond strength even without abrading the surface. All of the composite samples with HA showed higher strength. This could potentially be due to stiffening of the composite near the interface with the adherend.

The compressive modulus showed a decrease with HA content. Although HA has a higher modulus than the polymer, it did not effectively transfer the potential reinforcement effect possible for the composite. The observed variations in the pore structure could account for the lower modulus measured on a larger scale sample even if local properties of the material were higher. The overall compressive strength did not significantly decrease for the samples with HA inclusions, thus the HA is still a recommended addition because of the benefits of the larger and more interconnected pores for potential cell infiltration with the foam.

The chosen bovine bone test sections were solid cortical bone with no visible porosity and a flat surface. These sections represent the most challenging scenario for

bonding because it does not allow for mechanical interlocking with the adherend, but instead requires the intermolecular forces at the interface to bear the load. This makes proper wetting of the surface by the adhesive very important and in this system an amphiphilic primer proved to help overcome the surface energy mismatch with wet bone. In many existing studies on potential bone adhesive agents the bone surface was dry or it was not stated that wet conditions were maintained during the application of the adhesive to replicate conditions expected *in vivo* [14,17,21]. This mitigates the wetting and surface energy problem at the interface, which leads to higher adhesion strength results than would be achievable with wet conditions.

The surface primer used in this investigation was not optimized for use on bone material or for the adhesive used. However, the nearly twofold increase in strength that it promoted in our polymer and over fourfold increase with bone cement demonstrate the importance of this component in any adhesive system. Our adhesive showed a fourfold better adhesion on unmodified bone and nearly twofold better adhesion to primed bone compared with bone cement. This result is not unexpected because bone cement is intended to fill space and primarily uses mechanical interlocking with pores and friction to rigidly hold its placement against bone [13,17].

The bone to metal rod testing had a larger variation compared to the other testing methods. The variation was due in part to the difficulty of the test method. To obtain the tensile strength performance required careful control from the grips to ensure the bonded surface was perpendicular to the applied force. Any slight misalignment in the rod results in moments creating an asymmetric stress distribution across the bonded area and premature failure of the bond. Also the level of standard deviation can be high

when working with biological materials due to the inherent variations in geometry, chemical composition, and microstructure [13].

Biocompatibility tests showed osteoclast cells remodeling the outer damaged bone surface in all samples, and a significant halo of chondrocytes beginning the bone repair process. Some immune response is visible in the control frogs (Fig. 4.9. C and 4.9. D) and experimental frogs with the adhesive (Fig. 4.9. F and 4.9. H). There is degradation of damaged muscle fibers from the surgery and what appears to be some new fiber development. Most specimens with the adhesive showed a somewhat increased immune response compared to the control. However, any negative reactions appear to be localized to the immediate area of the adhesive, and no detrimental effects were observed near the distal or proximal ends away from the damage site. In addition to current tests we recognize that care should be taken in further assessments considering short-term observation does not always provide full biocompatibility conclusions, and the biocompatibility may vary with the species.

# CHAPTER 6

# CONCLUSIONS

## 6.1 SUMMARY

We studied a novel composite adhesive for bone-to-bone bonding applications, consisting of polyurethane foam matrix and reinforcing hydroxyapatite crystals. Despite the challenges, we consider the hydroxyapatite to still be an important part of the system. The calcium phosphate particles can improve osteoconductivity and increase initial spread of serum proteins compared to the polymer surface [8]. The increased interconnectivity of the pores observed in the sample prepared with HA would also be beneficial to cell migration and ingrowth. The addition of bioactive compounds should be further investigated for the ability of the adhesive system to potentially deliver bone growth factors to a fracture site. The results of these tests allowed us to well characterize the performance capabilities of the adhesive system, which are adequate for replacing screw fixation in many circumstances. The adhesive shows promise for performing in larger animal models for the purpose of bone bonding in a fracture stabilization study as a future step.

# CHAPTER 7

# ADDITIONAL APPLICATIONS

## 7.1 NANOINDENTATION TESTING

The elastic modulus of the matrix is important for any modeling of the composite system. Nanoindentation testing was used to obtain this parameter given the difficulty of obtaining a non-porous adhesive sample suitable for tensile testing. The nanoindentation was performed on a Hysitron TI 950 TriboIndenter with a Berkovich tip on both the adhesive and composite adhesive samples. To create the composite samples HA was added to a small amount of water and sonicated to disperse the nanoparticles. The polyurethane was then added at 7 parts polymer to 1 part water with shear mixing of the components while being sonicated for 1 minute. The adhesive was cured in small dishes and small areas without visible pores were selected for nanoindentation. The loading parameters were 5 second loading to 8 mN, a 10 second hold, and then a 2 second unload for all 5 indents on each sample (Table 7.2, 7.3). The elastic modulus of the polymer samples was calculated by the known relation to the measured reduced modulus.

$$\frac{1}{E_r} = \frac{\left(1-\nu_i^{\,2}\right)}{E_i} + \frac{\left(1-\nu_s^{\,2}\right)}{E_s} \tag{1}$$

A small difference was seen in the calculated modulus values, with a higher variation in the composite (Table 7.4). The particles in the composite adhesive are 200 nm and the loading is 1% by volume. The distance of the indents from underlying

particles could be significantly affecting the modulus measurements which would account for the higher variation seen in the composite sample.

## 7.2 MICROMECHANICS WITH BULK COMPRESSION SAMPLES

In order to obtain porosity estimates of the bulk compression samples micromechanics was applied using modulus data taken from the nanoindentation testing. To account for the HA particles the dilute approximation is used, with accompanying reasonable assumptions of linear elastic and isotropic spherical particles, a continuous linear elastic and isotropic matrix, and particle interaction is neglected, i.e. the concentration of particles is small, $c_2 << 1$. The equation for the effective composite bulk modulus $K_{eff}$ is readily obtained.

$$K_{eff} = \frac{K_1 + c_2(K_2 - K_1)(3K_1 + 4\mu_1)}{3K_2 + 4\mu_1} \tag{2}$$

The known relationship between the Poisson ratio $\nu$ and calculated elastic modulus $E$ to the bulk modulus $K$ and shear modulus $\mu$ provides all necessary inputs (Table 7.5).

$$K = \frac{E}{3(1-2\upsilon)} \tag{3}$$

$$\mu = \frac{E}{2(1+\upsilon)} \tag{4}$$

The predicted resulting change in the elastic modulus with the addition of 1% HA particles by volume is an increase from 1080 MPa to 1100 MPa. This theoretical prediction is in close agreement with the experimental composite modulus obtained through the use of nanoindentation (Table 7.4).

To account for the effect of the porosity in the bulk foam samples the Mori-Tanaka method was used. It assumes elastic spherical particles that are homogeneously dispersed in an elastic matrix, and both matrix and particles are isotropic in nature. The

equation for the effective foam bulk modulus is given by equation 5, with the assumed void bulk modulus $K_2 = 0$.

$$K_{foam} = \frac{K_1 + c_2(K_2 - K_1)K_1}{\left[\frac{3K_1}{3K_1 + 4\mu_1}\right](1 - c_2)(K_2 - K_1) + K_1} \tag{5}$$

This equation was then solved for $c_2$ to estimate the porosity of the foam. The predicted porosity to match the experimentally measured polyurethane modulus $E$ of 180 MPa corresponds to $c_2 = 69\%$. The polyurethane sample with HA, accounted for with the dilute approximation, predicts a porosity of $c_2 = 73\%$ to match the measured 150 MPa modulus $E$ in compression. Both of these values for porosity are within the range of that estimated for the foam samples.

The drawbacks of this method are that the volume fraction of pores may be getting too high for the Mori-Tanaka method, and there is some interconnectivity of pores. Additionally for the polymer sample with HA it was observed with SEM that the pores are in fact not spherical in shape which could further skew the predicted results.

| | | |
|---|---|---|
| Reduced modulus | $E_r$ | Measured |
| Indenter modulus | $E_i$ | 1140 GPa |
| Sample modulus | $E_s$ | Calculated |
| Indenter Poisson ratio | $\nu_i$ | 0.07 |
| Sample Poisson ratio | $\nu_s$ | 0.25 |

Table 7.1. Indentation parameters.

| Polyurethane Nanoindentation | | | |
|---|---|---|---|
| Test # | $H$ (MPa) | $E_r$ (MPa) | Contact Depth (nm) |
| 1 | 78.1 | 1150 | 2035 |
| 2 | 78.2 | 1156 | 2033 |
| 3 | 78.1 | 1151 | 2035 |
| 4 | 77.0 | 1144 | 2049 |
| 5 | 78.8 | 1159 | 2026 |
| Avg. | 78.0 | 1152 | 2036 |

Table 7.2. Hardness $H$, reduced modulus $E_r$, and contact depth from the indentation tests on polyurethane sample.

| Polyurethane with HA Nanoindentation | | | |
|---|---|---|---|
| Test # | $H$ (MPa) | $E_r$ (MPa) | Contact Depth (nm) |
| 1 | 65.1 | 1215 | 2230 |
| 2 | 64.1 | 1349 | 2247 |
| 3 | 64.7 | 1224 | 2237 |
| 4 | 59.5 | 1139 | 2334 |
| 5 | 58.3 | 1151 | 2356 |
| Avg. | 62.3 | 1216 | 2281 |

Table 7.3. Hardness $H$, reduced modulus $E_r$, and contact depth from the indentation tests on polyurethane with HA sample.

| Sample | Elastic Modulus |
|---|---|
| Pure adhesive | 1080 ± 5 MPa |
| Adhesive with HA | 1140 ± 77 MPa |

Table 7.4. Calculated polymer elastic moduli.

| | | |
|---|---|---|
| Polymer modulus | $E_1$ | 1080 MPa |
| HA modulus | $E_2$ | 120 GPa |
| Polymer Poisson ratio | $\nu_1$ | 0.25 |
| HA Poisson ratio | $\nu_2$ | 0.23 |

Table 7.5. Input parameters for micromechanics modeling.

# CHAPTER 8

# OVERVIEW OF MODELING

## 8.1 HETEROGENEOUS ADHESIVE MODELING

The modeling of many adhesive joints can be readily accomplished in commercial software such as Abaqus, given a number of restrictions. The systems that are well characterized include those that are 2 dimensional, and those with a homogeneous adhesive layer. The modeling challenges arise when the adhesive becomes a 3 dimensional multiscale heterogeneous material.

There are many different types of heterogeneous composite adhesives with varying microstructure that include a range of hard and soft particles. In particular the open issues in adhesive modeling include the development of a full 3D cohesive law framework verses current phenomenological approximations. The modeling of interfaces is usually done using cohesive law, but for heterogeneous systems the required cohesive law is not known because the traction separation law to use for the modeling of heterogeneous adhesives requires further study.

The development of the cohesive law for these types of inclusions will be necessary for the proper multiscale modeling of many types of adhesives. Until a cohesive law is developed, one solution in use is a multiscale model based on Hill's energy equivalence lemma used to couple the macro-scale and micro-scale in heterogeneous adhesives by constructing it computationally [22].

## 8.2 EXPERIMENTAL TESTING TO MODELING

The current need for more direct experimental support of developing cohesive models motivated establishment of the framework for the use of experimental data to develop and verify new adhesive models. This preliminary work has been done in collaboration with Dr. Karel Matous at the University of Notre Dame. The extensive adhesive modeling done by Dr. Matous provides an established basis for the experimental support in the advancement of heterogeneous adhesive modeling. The primary steps in this process are the experimental lap shear testing, a computed representative volume element, and finally the full lap shear model utilizing the new heterogeneous cohesive law (Fig. 8.1).

The process to achieve the unknown cohesive law for heterogeneous multiscale adhesives begins with the experimental lap shear test. The lap shear test provides the stress-strain curve for the actual adhesive up to the fracture point. Also with the use of acrylic adherend the samples can be imaged with a high-resolution digital camera or possibly with the use of a suitable micro-computed tomography (microCT) machine. This heterogeneous structure information for multiple samples can then be assembled and a representative volume element (RVE) can be constructed. If the polymer contains smaller particle inclusions, aside from the pores, then micromechanics can be used to homogenize the matrix material model.

Once a proper RVE is established periodic boundary conditions are applied on the four internal edges of the adhesive, and shear traction is applied to the top and bottom faces. The finite element modeling of the RVE allows the traction-displacement curve for the adhesive to be extended beyond the failure point of the experimental tests.

This full traction-displacement curve then provides the necessary input to generate the new cohesive law for a multiscale heterogeneous adhesive.

The new cohesive law can now be applied to cohesive elements in Abaqus. A full finite element model of the lap shear test including the adherend will be created incorporating the cohesive elements. Results from these simulations can then be checked against the experimental test data to verify the new cohesive law for a multiscale heterogeneous adhesive. With this the open issue in heterogeneous adhesive modeling of the development of a full 3D cohesive law framework instead of the current phenomenological approximations can be properly addressed.

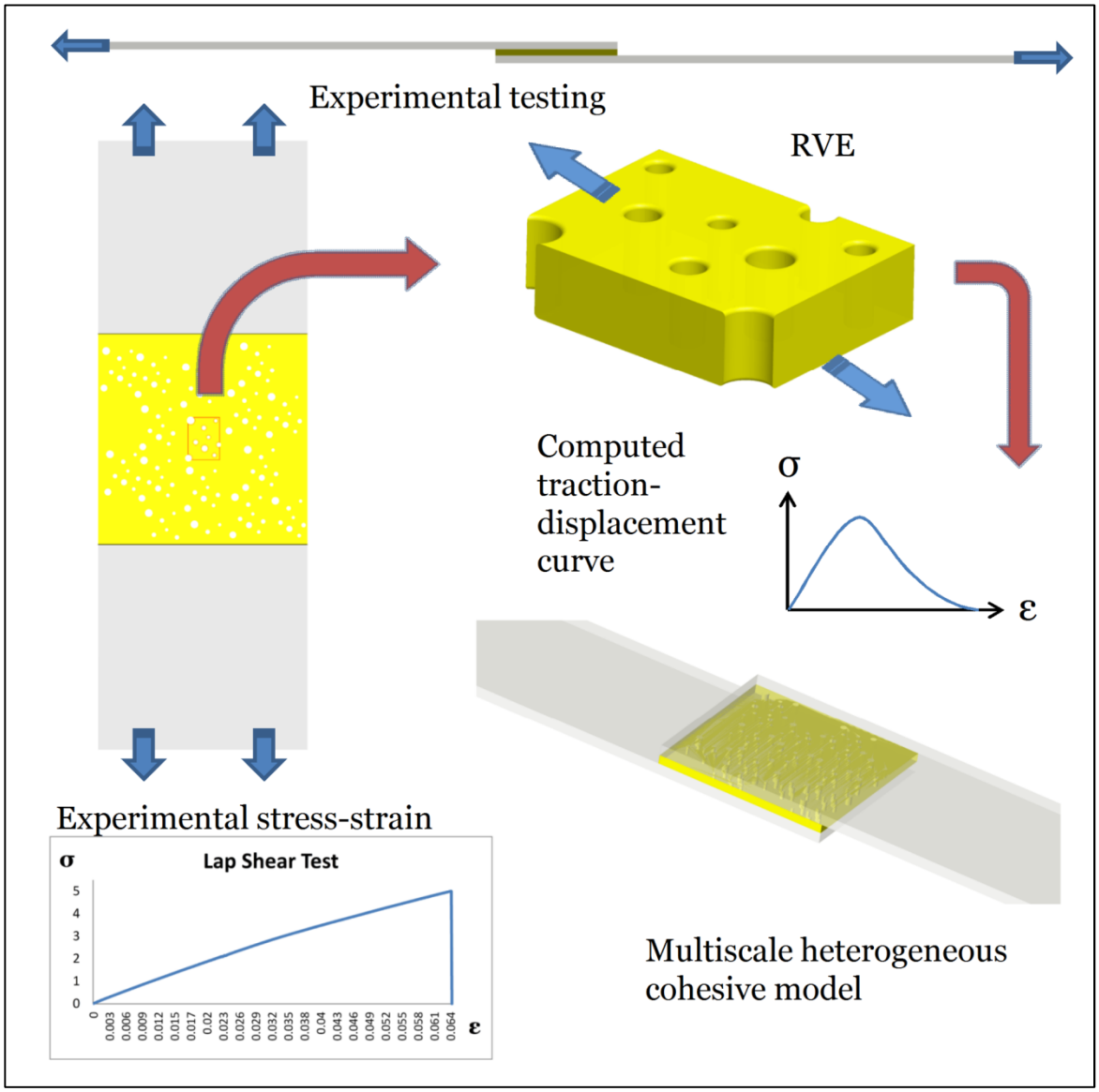


Figure 8.1. Diagram of progression of experimental data to the development of multiscale heterogeneous adhesive modeling.

## REFERENCES


1. Turusov R, Manevich L. Introduction to adhesion mechanics. Polymer Science Series D 2009;2:209-213.

2. T. E. Lipatova. Medical polymer adhesives. Biopolymers/Non-Exclusion HPLC, 1986. p. 65-93.

3. Heiss C, Kraus R, Schluckebier D, Stiller A, Wenisch S, Schnettler R. Bone Adhesives in Trauma and Orthopedic Surgery. European Journal of Trauma 2006;32:141-148.

4. Santerre JP, Woodhouse K, Laroche G, Labow RS. Understanding the biodegradation of polyurethanes: From classical implants to tissue engineering materials. Biomaterials 2005;26:7457-7470.

5. Eglin D, Mortisen D, Alini M. Degradation of synthetic polymeric scaffolds for bone and cartilage tissue repairs. Soft Matter 2009;5:938-947.

6. Guelcher S. Biodegradable Polyurethanes: Synthesis and Applications in Regenerative Medicine. Tissue Engineering Part B: Reviews 2008:3.

7. Guelcher S, Patel V, Gallagher K, Connolly S, Didier J, Doctor J. Synthesis and in vitro biocompatibility of injectable polyurethane foam scaffolds. Tissue Eng 2006;12:1247-1259.

8. Mano JF, Sousa RA, Boesel LF, Neves NM, Reis RL. Bioinert, biodegradable and injectable polymeric matrix composites for hard tissue replacement: state of the art and recent developments. Composites Sci Technol 2004;64:789-817.

9. Liu H, Zhang L, Zuo Y, Wang L, Huang D, Shen J, Shi P, Li Y. Preparation and characterization of aliphatic polyurethane and hydroxyapatite composite scaffold. J Appl Polym Sci 2009;112:2968-2975.

10. Guelcher S, Srinivasan A, Hafeman A, Gallagher K, Doctor J, Khetan S. Synthesis, In vitro degradation, and mechanical properties of two-component poly(ester urethane)urea scaffolds: Effects of water and polyol composition. Tissue Eng 2007;13:2321-2333.

11. Hamed E, Lee Y, Jasiuk I. Multiscale modeling of elastic properties of cortical bone. Acta Mech 2010.

12. Schortinghuis J, Bos RKM, Vissink A. Complications of internal fixation of maxillofacial fractures with microplates. Journal of Oral and Maxillofacial Surgery 1999;57:130-134.

13. Endres K, Marx R, Tinschert J, Wirtz D, Stoll C, Riediger D, Smeets R. A new adhesive technique for internal fixation in midfacial surgery. BioMedical Engineering OnLine 2008;7:16.

14. Maurer P, Bekes K, Gernhardt CR, Schaller H-, Schubert J. Comparison of the bond strength of selected adhesive dental systems to cortical bone under in vitro conditions. Int J Oral Maxillofac Surg 2004;33:377-381.

15. Shermak M, Wong L, Inoue N, Crain B, Im M, Chao E. Fixation of the craniofacial skeleton with butyl-2-cyanoacrylate and its effects on histotoxicity and healing. Plastic and reconstructive surgery 1998;102:309-318.

16. Grossterlinden L, Janssen A, Schmitz N, Priemel M, Pogoda P, Amling M. Deleterious tissue reaction to an alkylene bis(dilactoyl)-methacrylate bone adhesive in long-term follow up after screw augmentation in an ovine model. Biomaterials 2006;27:3379-3386.

17. Smeets R, Riediger D, Wirtz D, Marx R, Endres K. Partially adhesive fixation of reconstruction plates at midfacial fractures - An alternative solution to screw fixation? Materialwissenschaft und Werkstofftechnik 2007;38:178-180.

18. Hafeman A. Local delivery of tobramycin from injectable biodegradable polyurethane scaffolds. Journal of biomaterials science.Polymer edition 2010;21:95-112.

19. Kricheldorf HR, Nuyken O, Swift G. Handbook of polymer synthesis. 2nd ed. New York: Marcel Dekker, 2005.

20. Feng L, Milner D, Xia C, Nye H, Redwood P, Cameron JA, Stocum D, Fang N, Jasiuk I. Long Bone Critical Size Defect Repair by Regeneration in Adult Xenopus Laevis Hind Limbs. Tissue Engineering Part A In Revision.

21. Perry M, Youngson C. In-vitro fracture fixation - Adhesive systems compared with a conventional technique. The British journal of oral maxillofacial surgery 1995;33:224-227.

22. Kulkarni MG, Matous K, Geubelle PH. Coupled multi-scale cohesive modeling of failure in heterogeneous adhesives. Int J Numer Methods Eng 2010.